JOURNAL OF
Materials
CHEMISTRY

Formation of mesoporous, zirconium(IV) oxides of controlled surface areas

Philippe Trens,[a] Michael J. Hudson*[a] and Renaud Denoyel[b]

[a] *Department of Chemistry, University of Reading, PO Box 224, Whiteknights, Reading, Berkshire, UK RG6 6AD*

[b] *Centre de Thermodynamique et de Microcalorimétrie du CNRS, CTM, 26 rue du 141ème RIA, 13003 Marseille, France*

Control of the surface areas of the calcined zirconium(IV) oxides arises from the extent of equilibration permitted between the hydrolysed zirconyl oxychloride and the surfactant prior to calcination. The properties of the zirconia–surfactant materials, which are formed by a scaffolding and controlled drying mechanism, and the subsequent oxides obtained on calcination depend more on the times allowed for equilibration than on the ratios of zirconia:surfactant. During the equilibration over *ca.* 24 hr between the hydrolysing zirconium oxychloride and CTAB, the small, unstable zirconium oxide particles mix intimately with the surfactant. These particles recrystallise (and loosely aggregate) on calcination to give tetragonal zirconias of intermediate surface areas (50 $m^2 g^{-1}$). Equilibration over 90 h gives thermally stable (up to 450 °C), small (<100 Å) tetragonal zirconia nanoparticles which maintain their integrity after calcination to give high surface area materials.

Introduction

Zirconium oxide itself is known to have useful ion exchange properties but there is a requirement to improve its thermal stability.[1,2] In addition, zirconium oxide finds wide application both as a catalyst support and as a catalyst when sulfated.[3–5] However, in order to improve the catalytic and general properties particularly of zirconias, high surface area pure zirconias, which do not have additional stabilisers such as yttrias, phosphates, silicas or sulfates, are required. In a previous publication, we have shown that high-surface-area, mesoporous zirconium(IV) oxides may be prepared by the equilibration of zirconium oxychloride with cationic surfactants such as cetyltrimethylammonium bromide (CTAB) followed by calcination.[6] The BET surface areas of the calcined materials varied from 240–360 $m^2 g^{-1}$ and compared favourably with those of calcined aerogels. The overall mechanism for the preparation of these materials suggested that the surfactant reduces the surface tension differences between the inorganic and organic phases and also serves as a controlled drying and scaffolding agent (*i.e.* a support for the inorganic framework) at temperatures below 570 K prior to the calcination between 723 and 973 K. However, in this earlier study, the nature of the zirconia–surfactant material and the possibilities of controlling the surface areas of the zirconium–surfactant materials and the calcined zirconias were not studied. The above scaffolding mechanism has been extended to include the synthesis of mesoporous zirconias with anionic surfactants.[7]

Frequently, in order to prepare mesoporous zirconias, an additional anion such as phosphate or sulfate must be present. Calcination of precursors without such anions often leads to a disordered zirconia of low surface area. It has been shown, for example, that mesoporous zirconia, which contains phosphate as the structure-building anion, may be prepared by hydrolysis of zirconium propoxide in the presence of $C_{12}H_{25}OP(OH)_2$ and subsequent calcination. The authors claim that the particle diameters, 4–10 µm, did not appear to influence the sintering stage during calcination. The corresponding sulfate analogue did not yield a mesoporous material since calcination caused the conversion of the tetragonal form to the monoclinic phase.[8] This is in contrast with the observations by Sachtler and coworkers who found that sulfation of the precursor formed using acidified primary amine, and subsequent calcination, led to a stable mesoporous material, from which a tetragonal form developed at about 600 °C.[9] The stability of the tetragonal zirconia appears to be driven by particle size.[10–12] Thus the apparent discrepancies between the studies may simply be a question of the particle sizes prior to calcination. At 500 °C, particles with diameters greater than 16 nm appear to undergo the tetragonal to monoclinic transformation.[13] Those with smaller particle sizes remain in the tetragonal phase. Cohydrolysis of silicon and zirconium alkoxides in the presence of surfactants allows the formation of mesoporous oxides in which the zirconia is an integral part of the structure.[14] However, the additional oxide (or anion) changes the properties of the zirconium oxide itself. For example, it has been shown that incorporation of zirconium oxides in silicas produces materials which are catalysts for liquid phase peroxidations. However, the oxide itself is not catalytically active, either because the micropores are too small or because of the proximity of the zirconium atoms in the oxide itself.[15] There is clearly an urgent requirement to prepare pure zirconias of controlled surface areas, which do not contain additional anions or oxides that modify the properties of the pure zirconias.

Experimental

Preparation

The general scheme for the preparation of the calcined oxides has been previously described by Hudson and Knowles[6] Typically, to an aqueous solution of $ZrOCl_2 \cdot 8H_2O$ (0.1 mol l^{-1} in zirconium, 100 cm^3, Aldrich) was added an aqueous solution of cetyltrimethylammonium bromide (CTAB) (25% by mass, 100 cm^3, Aldrich) leading to a zirconium oxide:surfactant ratio of 1:10. This combined solution was then stirred for 15 min (pH = 1.15) and then NaOH (1 M, Aldrich) was added until the pH reached 11.6 at which the mixture was maintained throughout. The mixture was then stirred at room temperature for 60 min in a closed polypropylene bottle and then placed in a thermostatically controlled water-bath at 363 K. The reaction mixture was allowed to equilibrate for either 24 h or for 90 h, and then after this time, the mixture was allowed to cool, the solid was filtered off under suction and washed extensively with distilled water until free of unbound surfactant

Table 1 Samples prepared in this work

	(ZrO_2;0.1;90)	(ZrO_2;2;90)	(ZrO_2;0.1;24)[a]	(ZrO_2;2;24)[a]
Zr/CTAB molar ratio	1:10	2:1	1:10	2:1
reaction time/h	90	90	24	24

[a] Other materials equilibrated for 6 and 18 h, for example, had very similar properties.

and sodium ions. The white powder was oven dried at 353 K for 5 h. The concentration of the cetyltrimethylammonium bromide (CTAB) was altered in some experiments to 0.1 mol l^{-1}, leading to a zirconia–surfactant ratio of 2:1. The differences between four typical syntheses are summarised in the Table 1. As indicated in the text and the captions, other times of equilibration have been investigated.

Calcination of the materials

The materials were calcined in static air up to 773 K for 5 h at a ramp rate of 5 K min^{-1}. The ramp-rate (1–15 K min^{-1}) did not appear to have a significant effect on the properties of the calcined materials. After calcination, the materials were allowed to cool in the furnace itself until room temperature was reached. Chemical analysis showed that there was no (<0.1%) sodium, carbon or silica in the samples discussed.

Characterisation

Both uncalcined and calcined materials were heated to 413 K for 2 h under nitrogen flow in order to remove the physisorbed water prior to nitrogen adsorption measurements. The nitrogen adsorption isotherms were determined at 77 K by means of a Micromeritics Gemini 2370 surface area analyser. All adsorption experiments were performed at least in duplicate. Surface areas were derived from the BET equation[16] in the relative pressure range 0.05–0.35 assuming a cross-sectional area of 0.162 nm^2 for the nitrogen molecule. The mesopore size distributions were calculated from the desorption branch by the BJH method.[17] The water adsorption isotherms were determined at 298 K by means of a magnetic compensation adsorption balance which was made in Marseille. All of the gas volumes quoted have been corrected to standard temperature and pressure. The samples were also studied using X-ray powder diffraction (XRD) with a Spectrolab CPS Series 3000 120, using Ni-filtered Cu-Kα radiation. For the tetragonal phase, the details were (111) 30.29°; (200) 35.22°; (220) 50.43°; (310) 60.31°; (222) 81.91°; (400) 95.36°. There was never any evidence for a monoclinic phase. Thermogravimetry–differential thermal analysis (TG–DTA) was carried out using a Stanton-Redcroft STA 1000 instrument with lidless, platinum pans, with recalcined alumina as the DTA reference. Transmission electron micrographs were recorded on a JEOL-JEM 200 CX instrument at 200 kV.

Results and Discussion

The hydrolysis of zirconyl oxychloride has been previously studied in the absence of surfactants. It has been shown, for example, that the principal hydrolysing species is the tetramer $[Zr(OH)_2 \cdot 4H_2O]_4^{8+}$.[18] The mechanisms involving the tetramer have been confirmed by electron microscopic studies of the hydrolysis of zirconyl chloride.[19] With respect to the formation of the tetragonal phase, the platelets derived from the tetramer stack in a regular manner (see Fig. 9).

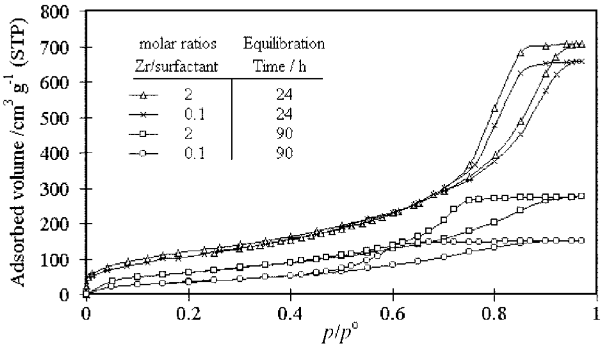

Fig. 1 Adsorption isotherms of nitrogen at 77 K on the uncalcined samples

Zirconia–surfactant (uncalcined) materials

Equilibration of the hydrolysed zirconyl chloride and the CTAB produced zirconia–surfactant materials, which had interesting properties in their own rights. Fig. 1 shows the adsorption isotherms of nitrogen at 77 K for these uncalcined materials. The shapes of all these curves are of type IV according to the IUPAC classification indicating mesoporosity.[20] The hysteresis loops are, in each case, at high relative pressures indicating a rather wide range of pore diameters.

The saturation plateaux at high relative pressures (*e.g.* $p/p^\circ > 0.9$ for samples ZrO_2;2;24 and ZrO_2;0.1,24) are well defined but suggest that the mesoporosity could arise between particles. The specific surface areas, the C_{BET} parameters and the total pore volumes are reported in Table 2.

Interestingly, the two uncalcined materials from the 24 h equilibration (together with materials prepared over 6 or 18 h) have similar high surface areas, pore volumes and type IV adsorption isotherms but which are quite different from those obtained after 90 h equilibration. Clearly, the dominant factor here is the length of the time of equilibration rather than the ratio of the zirconia to the surfactant used. The C_{BET} values, which relate to the interaction between the adsorbate nitrogen and the adsorbent, are rather similar, however, but are all lower than would be expected for mesoporous inorganic oxide materials, values for which have been found to be in the range 70–100. The values confirm a close interaction between the zirconia and the surfactant, and suggest that the hydrophobic surfactant coating of the particles leads to weaker interactions with the nitrogen molecules than is the case with the calcined materials. The uncalcined materials obtained after 90 h equilibration each have surface areas in the region of 145–220 m^2 g^{-1} which, whilst still high, are lower than those values for the materials obtained after 24 h equilibration.

Fig. 2 shows BJH pore size distribution plots for the uncalcined materials calculated from the desorption branch of the adsorption isotherms. The results for experiments in which the shorter times of 8, 12 and 24 h were similar to each other but different from those with longer equilibration time 90 h material. The pore size distributions may be attributed to a percolation effect of the nitrogen molecules between particles of different sizes at relative pressures down to 0.42. Although the pore distributions are not sharp, the peaks are reasonably well defined in the mesoporous range. Such porosities are not evident in the mesophases for the (ordered) templated MCM materials but are characteristic of the 'scaffolded' (more disordered) zirconia-surfactant intermediates. Nevertheless, it is interesting that all of these materials are mesoporous and of high surface area so that they have potential for application as sorbents for hydrophobic substances, which could lead to efficient remediation of contaminated effluent streams.[21]

Fig. 3 shows typical TG–DTA (thermogravimetry and differential thermal analysis) curves obtained with each of the zirconia–surfactant materials. It is possible to identify the

Table 2 Specific surface areas (S_{BET}), C_{BET} and total pore volumes for the uncalcined materials (unc) and the calcined materials (cal)

	ZrO_2;0.1;90		ZrO_2;2;90		ZrO_2;0.1;24[a]		ZrO_2;2;24[a]	
material	unc	cal	unc	cal	unc	cal	unc	cal
S_{BET}/m^2 g^{-1}	145	266	217	326	450	40	415	47
C_{BET}	50	55	30	70	50	(1000)	45	(500)
V_p/cm^3 g^{-1}	0.23	0.32	0.42	0.56	1.08	0.28	1.09	0.28

[a] Also 8 and 12 h; estimated values are given in parentheses.

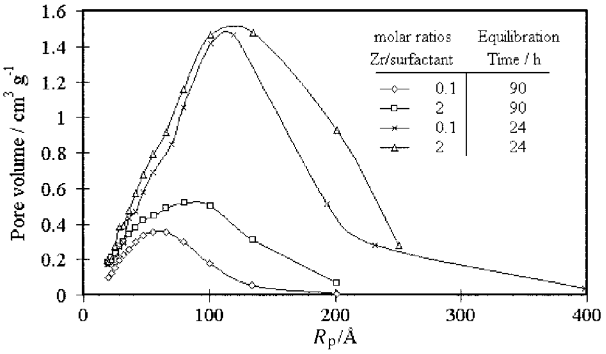

Fig. 2 BJH pore size distribution plots for the uncalcined materials calculated from the desorption branch of the adsorption isotherms

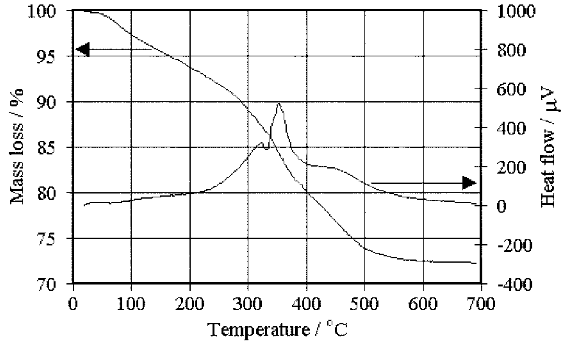

Fig. 3 Typical TG–DTA (thermogravimetry and differential thermal analysis) curves obtained with each of the zirconia–surfactant materials

removal of water between 50 and 100 °C from the endotherm on the DTA curve. There is a steady removal of water up to 250 °C, consistent with a controlled drying mechanism. From 250–500 °C, the degradation of the zirconia–surfactant material takes place in several steps with the main decomposition corresponding to oxidation of the surfactant being at 350 °C. The 'pore' hydroxyl groups are removed from the structure by dehydroxylation as shown by the clear endotherm at 320 °C. These results are consistent with TG–DTA studies on silicas such as Spherosil, which are known to have internal hydroxyl groups that are involved in dehydroxylation reactions at similar temperatures.[22] An important feature to note is that the structure of the inorganic part is fixed by 320 °C, *i.e.* prior to removal of the surfactant and the subsequent calcination at 450 °C. Thus the overall morphology of the subsequently calcined material is largely governed by that of the inorganic part in the zirconia–surfactant material prior to calcination.

Calcined zirconias

Fig. 4 shows the adsorption isotherms of nitrogen at 77 K for the calcined materials. In both of the samples heated for 90 h, the shapes of the two adsorption isotherms are similar to those previously determined for the inorganic–organic intermediates prior to calcination, suggesting that the mechanism involving the percolation of nitrogen during adsorption and desorption has not changed significantly. In effect, the structure was stabilised during the controlled drying during the longer equilibration time probably involving dehydroxylation reactions within and between the layers. Such dehydroxylation reactions have been shown to proceed below 100 °C.[23] The affinities of nitrogen for the two samples is similar, as is evidenced by the position of the 'knees', the initial slopes and similar C_{BET} values, Table 2. The specific surface areas are also much higher than those previously obtained for the precipitation of zirconia in the absence of the surfactant by Gimblett *et al.*[24] The values also compare favourably with those obtained for calcined materials obtained from aerogels.[24] Further information may be gleaned from the isotherms. For example, mesoporous compounds have been obtained by the hydrolysis of zirconyl chloride in the presence of sodium hydrogencarbonate at pH 7 and out-gassing at 450–660 °C. The isotherms for these materials are very similar to those considered here. Narrow mesopores were formed by the loss of water at low temperatures and wider mesopores were formed above 300 °C by the decomposition of the carbonate.[25] These materials, therefore, contain narrow and wide mesopores. Capillary condensation occurs in both sets of mesopores, but for the wider pores occurs at higher relative pressures.[26] For the materials under study here, the surfactant controls the dehydration and the scaffolding such that the amount of small pores is greatly restricted. The principal part of the mesopores is formed when decomposition of the surfactant occurs at 320–370 °C. Pores are essentially present in the structure but are blocked by the surfactant.

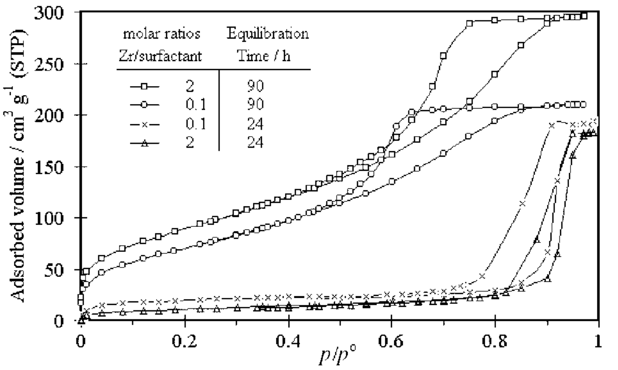

Fig. 4 Adsorption isotherms of nitrogen at 77 K for the calcined materials

The shapes of the adsorption isotherms for the samples equilibrated for only 24 h, however, are quite different before and after calcination. For the calcined materials, the hysteresis loops occur at high relative pressures of *ca.* 0.9, but still may be attributed to the filling of mesopores because of the flat plateau between $p/p^0 = 0.90$ and $p/p^0 = 0.99$. The loop is sharp and steeply inclined suggesting a wide range of mesopores. The surface areas decreased significantly upon calcination owing, as discussed later, to the formation of tetragonal zirconia. Although the C_{BET} values are difficult to quantify, it is clear that they are significantly increased suggesting, when coupled with decreased pore volumes, that a significant amount

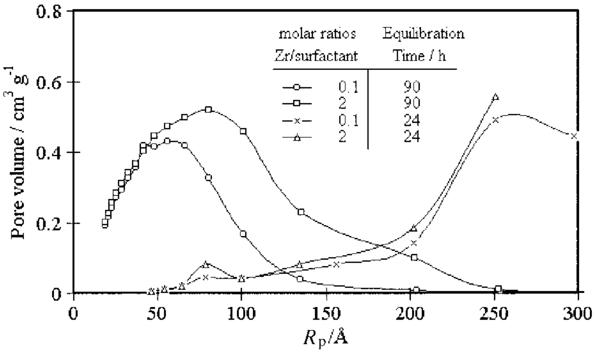

Fig. 5 Pore size distributions according to the BJH method calculated from the desorption branches for the calcined materials

of crystallisation of the compound occurred during calcination, Table 2.

Fig. 5 shows the pore size distributions according to the BJH method calculated from the desorption branches for the calcined materials. The samples calcined after 90 h equilibration show clearly defined pores of *ca.* 5 and 7 nm (50 and 70 Å). The calcined materials obtained after 24 h equilibration are quite different since there is a small peak at *ca.* 17 nm that can be related to the percolation effect suggesting that there is an aggregation of small particles.

XRD powder diffraction

The lower two curves in Fig. 6 show the XRD powder diffraction patterns for the uncalcined samples. For each sample there is a broad single peak ($2\theta = 2.3$, which corresponds to a distance of 38–40 Å), which could be ascribed to a hexagonal arrangement as seen in an MCM-41-type material. However, there could also be a regular arrangement of wormholes within the particles. Assemblies of mesoporous molecular sieves have been prepared which contain wormhole structures with uniform channel diameters over a range comparable to M41S materials.[27] These structures lack regular channel packing.

Fig. 6 also shows, in the upper two curves, the XRD powder patterns for the calcined samples. For the samples obtained after the longer (90 h) equilibration, there is little change in the pattern from that of the uncalcined materials. However, those materials obtained after only 24 h equilibration had XRD powder patterns after calcination which were characteristic of tetragonal zirconia. This observation is consistent with the high values of C_{BET} for these materials and the significant lowering of the surface areas. The degree of lowering of the surface areas for these materials may be related to the extent of recrystallisation to form the tetragonal phase, suggesting that the surface areas may be controlled according to the amount of recrystallisation that is allowed. The equilibration time at the first stage permits a convenient control over the ordering of the platelets. At no time was the monoclinic phase observed suggesting that, even though there was some agglomeration of particles (Fig. 8), the particle sizes were below 16 µm.[18]

Fig. 7 refers to the adsorption isotherms of water at 295 K for the uncalcined and calcined (ZrO_2;2;90) material. Prior to calcination, the material shows an isotherm which is clearly not related to a well defined mesoporous material, being essentially related to the hydrophobic regions of the surfactant. On the other hand, the isotherm for the calcined material is rather similar to that for nitrogen and may be classified as a type IV isotherm typical of mesoporous materials with a wide

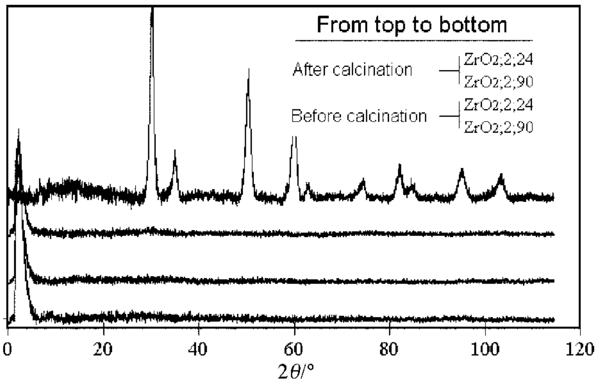

Fig. 6 The lower two curves show the XRD powder diffraction patterns for the uncalcined samples; the upper two curves show the XRD powder patterns for the calcined samples

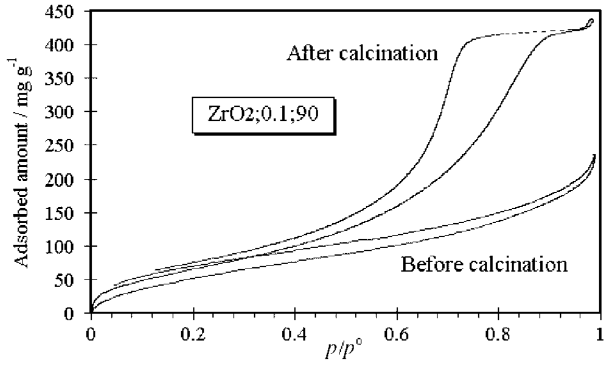

Fig. 7 Adsorption isotherms of water at 295 K for the uncalcined and calcined (ZrO_2;2;90) material

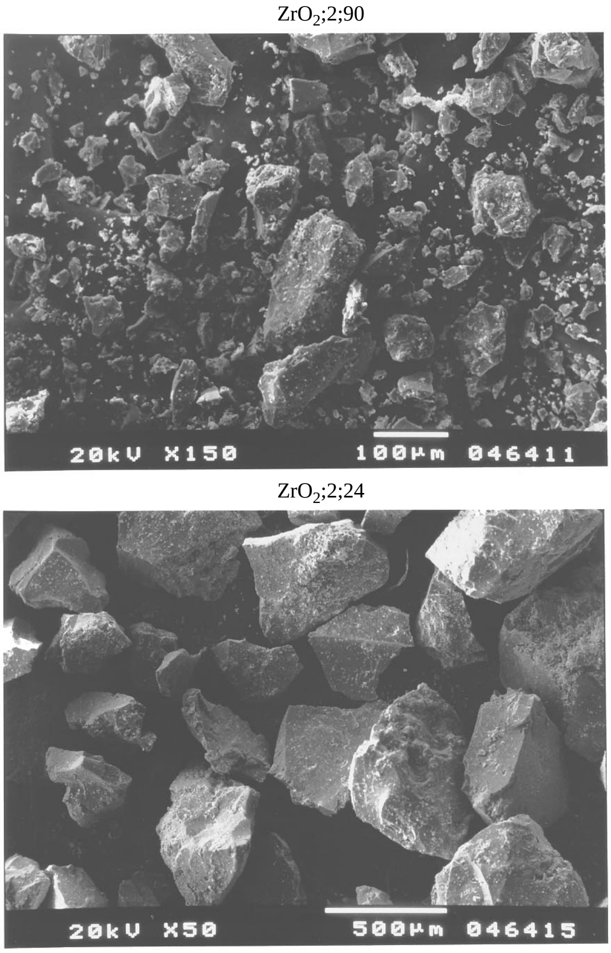
ZrO_2;2;90

ZrO_2;2;24

Fig. 8 Scanning electron micrographs for the calcined ZrO_2;2;90 and the ZrO_2;2;24 material

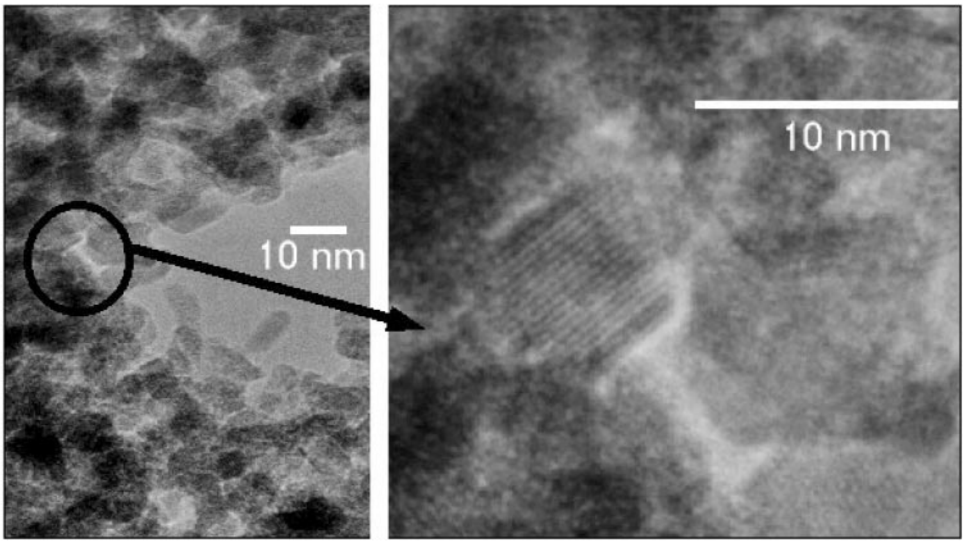

Fig. 9 Two transmission electron micrographs of the calcined ZrO_2;2;90 material

range of pores. There is probably some rehydroxylation between the water and the zirconia since the hysteresis curve is not closed.

The top micrograph in Fig. 8 shows the scanning electron micrographs for the calcined $ZrO_2:2:90$ material; it can be seen that there are irregular (loosely bound) aggregates ranging from 1–100 μm. On the other hand, the ZrO_2;2;24 material, for example, has much larger aggregates, typically 300–500 μm. Thus the extent of aggregation of the particles resulting from the calcination is related to the equilibration times.

Fig. 9 shows two transmission electron micrographs of the calcined ZrO_2;2;90 material. Small particles of <100 Å can be identified in the left hand image. Interestingly, in the right hand image (a magnification of the left hand image), there are clearly some crystalline regions which could correspond to the tetragonal phase observed for the ZrO_2;2;24 material. Thus the apparent lack of XRD peaks for this material is related to the very small particles size and not to an amorphous nature.

Under the basic conditions used here, the initial hydrolysis of the zirconium oxychloride is rapid which normally leads to the monoclinic phase. Surfactants permit the organisation of the zirconias through controlled dehydration and scaffolding.[6] The surfactants envelope the hydrolysing zirconia and control diffusion between the zirconia regions.[28] After 24 h, the particles of zirconia, which may contain platelets derived from the tetramer, are rather unstable and recrystallise on calcination to form particles which are sufficiently large to enable the tetragonal phase to be identified by XRD. Between 24 and 90 h, the particles of zirconia become more stable owing to dehydroxylation particularly at the layer edges, (even without additional anions such as sulfate or phosphate), and remain very small so that they are essentially X-ray amorphous. Calcination removes the surfactant and leaves stable particles of tetragonal zirconia of high surface area. The porosity arises from the intraparticular or textural properties of the materials. By the means described above, therefore, it is possible to prepare tetragonal zirconias of different, controlled surface areas.

Conclusions

This study shows that it is possible to synthesise pure, mesoporous tetragonal zirconia oxides, *i.e.* without additional stabilisers, using surfactants to control the stacking of the platelets, particle sizes and stabilities. Moreover, the times for equilibration between the zirconium oxychloride and the surfactant allow some degree of control of the surface areas not only of the zirconia–surfactant materials but also the subsequent calcined materials. Equilibration for 8, 12 and 24 h leads to mesoporous zirconia–surfactant materials of high surface areas and pore volumes. These contain zirconia particles, which are unstable on calcination, so that they recrystallise and aggregate to form tetragonal zirconias of lower surface areas. Over longer times of equilibration (90 h), the small particles (<100 Å) formed lead to high surface area, tetragonal zirconias on calcination.

We wish to thank the European Commission under the Training and Mobility of Researchers (TMR) Programme for funding this work under grant number ERB FM RX 960084.

References

1 A. Clearfield, *Inorg. Chem.*, 1964 **3** 146.
2 M. Turrillas, P. Barnes, D. Gascoigne, J. Z. Turner, S. L. Jones, C. J. Norman, C. F. Pygall and A. J. Dent, *Radiat. Phys. Chem.*, 1995, **45**, 491.
3 A. Corma, *Chem. Rev.*, 1997, **97**, 2373.
4 R. Franklin, *Catal. Today* 1991, **10**, 405.
5 B. H. Davis, *Catal. Today*, 1994, **20**, 220.
6 M. J. Hudson and J. A. Knowles, *J. Mater. Chem.*, 1996, **6**, 89.
7 G. Pachero, E. Zhao, A. Garcia, A. Skylarov and J. J. Fripiat, *J. Mater. Chem.*, 1998, **8**, 219.
8 G. Pacheco, E. Zhao, A. Garcia, A. Skylarov and J. J. Fripiat, *Chem. Commun.*, 1997, 491.
9 Y.-Y. Huang, B. Y. Zhao and Y. C. Xie, *Appl. Catal A: General*, 1998, **171**, 75.
10 R. G. Garvie, *J. Phys. Chem.*, 1978, **82**, 219.
11 H. Saha, S. K. Dutta, S. M. Hassain, S. Chakraborty and A. Saha, *Bull. Mater. Sci.*, 1998, **21**, 195.
12 C. R. Aita, M. D. Wiggins, R. Whig, C. M. Scanlan and M. Gajdardziska-Josifovska, *J. Appl. Phys.*, 1994, **79**, 1176.
13 M. Gajdardziska-Joisfovska and C. R. Aita, *J. Appl. Phys.*, 1994, **79**, 1315.
14 D. J. Jones, J. Jiménez-Jiminez, A. Jiménez-Lopez, P. Maireles-Torres, P. Olivera-Pastor, E. Rodriguez-Castillón and J. Rozière, *Chem. Commun.*, 1997, 431.
15 A. Tuel, S. Gontier and R. Teissier, *Chem. Commun.*, 1996, 651.
16 S. Brunauer, P. H. Emmett and E. Teller, *J. Am. Chem. Soc.*, 1938, **60**, 309.
17 E. P. Barrett, L. G. Joyner and P. P. Halenda, *J. Am. Chem. Soc.*, 1951, **73**, 373.
18 A. Clearfield, *J. Mater. Res.*, 1990, **5**, 161.
19 J. L. Fryer, *J. Colloid Interface Sci.*, 1976, **34**, 132.

20 K. S. W. Sing, D. H. Everett, R. A. W. Haul, L. Moscou, R. A. Pierotti, J. Rouquerol and T. Siemieniewska, *Pure Appl. Chem.*, 1985, **57**, 603.

21 L. Mercier and T. J. Pinnavaia, *Adv. Mater.*, 1997, **9**, 500.

22 K. K. Unger, *J. Chromatogr. Libr.*, 1979, **16**, 76.

23 D. C. Apperley, M. J. Hudson, M. T. J. Keene and J. A. Knowles, *J. Mater. Chem.*, 1995, **5**, 577.

24 S. S. Prakash, C. J. Brinker, A. J. Hurd and S. M. Rao, *Nature*, 1995, **374**, 349.

25 F. G. R. Gimblett, A. A. Rahman and K. S. W. Sing, *J. Colloid Interface Sci.*, 1984, **102**, 483.

26 S. J. Gregg and K. S. W Sing, *Adsorption*, *Surface Area and Porosity*, Academic Press, London 1982, 2nd edn., p. 163.

27 E. Prouzet and T. J. Pinnavaia, *Angew. Chem.*, 1997, **36**, 516.

28 *Design of New Materials*, ed. D. L. Locke and A. Clearfield, Plenum, New York, 1986.

Paper 8/05193C; *Received* 6*th July*, 1998